

**Activation of metabotropic glutamate receptor 1 dimers requires
glutamate binding in both subunits*.**

Paul J. Kammermeier* and June Yun,

Department of Physiology and Pharmacology, Northeastern Ohio Universities College of
Medicine (NEOUCOM), Rootstown, OH 44272.

Running title: Intradimer crosstalk in mGluR1.

*Corresponding author: Paul J. Kammermeier, Ph.D.

Department of Physiology and Pharmacology,
Northeastern Ohio Universities College of Medicine,
4209 State route 44, P.O. Box 95

Rootstown, OH 44272

Phone: 330-325-6530

Fax:330-325-5912

pjkammer@neoucom.edu

of pages:

of tables: 0

of figures: 7

of references: 26

Words in *Abstract*: 244

Words in *Introduction*: 585

Words in *Discussion*: 1492

Abbreviations: mGluR: metabotropic glutamate receptor; Glu: glutamate; GPCR: G protein coupled receptor; WT: wild type.

Recommended section: Cellular and molecular.

ABSTRACT

Group I metabotropic glutamate receptors (mGluRs) form stable, disulfide-linked homodimers. Lack of a verifiably monomeric mGluR1 mutant has led to difficulty in assessing the role of dimerization in the molecular mechanism of mGluR1 activation. The related GABA_B receptor exhibits striking intradimer crosstalk (ligand binding at one subunit effectively produces G protein activation at the other), but it is unclear whether group I mGluRs exhibit analogous crosstalk. Signaling of heterologously expressed mGluR1 was examined in isolated rat sympathetic neurons by measuring glutamate-mediated inhibition of native calcium currents. To examine mGluR1 activity when only one dimer subunit has access to glutamate ligand, wild type mGluR1 was coexpressed with mGluR1 Y74A, a mutant with impaired glutamate binding, and the activity of the 'heterodimer' (mutant/wild type) was examined. The mGluR1 Y74A mutant alone had a dose response curve that was shifted by about 2 orders of magnitude. The half maximal dose of glutamate shifted from 1.3 μ M (wild type mGluR1) to about 450 μ M (mGluR1 Y74A). However, the maximal effect was similar. Wild type mGluR1 was expressed with excess Y74A mGluR1 to generate a receptor population consisting largely of mutant homodimers and mutant/wild type heterodimers but without detectable wild type homodimers. Under these conditions, no glutamate mediated calcium current inhibition was observed below \sim 300 μ M glutamate, although wild type mGluR1 protein was detectable with immunofluorescence. These data suggest that mutant/wild type heterodimeric receptors are inactive at ligand concentrations favoring glutamate association with receptor dimers at only one subunit.

Running title: mGluR1 dimer activation requires both subunits.

INTRODUCTION

Metabotropic glutamate receptors (mGluRs) belong to family 3 of the heptahelical G protein-coupled receptor (GPCR) superfamily (Kaupmann et al., 1997). Eight mGluR genes, mGluR1-8, have been identified and categorized into three groups, I-III, based on sequence homology and pharmacology (Nakanishi, 1994; Pin and Duvoisin, 1995; Conn and Pin, 1997). Group I mGluRs (mGluR1 and 5) form stable homodimers (Romano et al., 1996; Robbins et al., 1999).

Of the family 3 G protein coupled receptors, dimerization of GABA_B receptors has been best characterized. The GABA_B receptor is an obligate heterodimer comprised of two subunits, GBR1 and GBR2 (Margeta-Mitrovic et al., 2000). GBR1 contains an endoplasmic reticulum (ER) retention signal that prevents insertion into the plasma membrane unless bound to GBR2 (Margeta-Mitrovic et al., 2000). GBR2 alone is unable to bind GABA. The N-termini of GBR1 and 2 must be present for the receptor to function properly (Margeta-Mitrovic et al., 2001b). However, G protein activation occurs largely through the GBR2 subunit (Margeta-Mitrovic et al., 2001a; Robbins et al., 2001). Thus, there is precedent for heterodimerization in the heptahelical GPCR family 3, and for molecular crosstalk between individual dimer partners.

Structural studies on the ligand binding, N-terminal region of mGluR1 have led to a model of activation wherein each subunit of mGluR1 receptor dimers forms a clamshell-like structure (Kunishima et al., 2000). Orientation of dimer subunits with respect to each other can shift around a dimer interface region to induce a conformational change presumably leading to receptor activation. These possible structural conformations are in equilibrium such that in the absence of ligand, the so-called 'open-open/R' (resting) conformation is favored. In the presence of ligand, receptors are active due to an equilibrium shift to the 'open-closed/A' or 'closed-closed/A' conformations, depending at least in part on the presence of stabilizing di- or trivalent cations (Tsuchiya et al.,

2002). Finally, a recent study has suggested that full activity of mGluR1 dimers is achieved only in the closed/closed conformation (Kniazeff et al., 2004).

Despite this progress, the molecular mechanism of receptor activation of mGluR1 remains unclear. The structural studies suggest that glutamate binds both dimer subunits similarly (Kunishima et al., 2000; Tsuchiya et al., 2002). Glutamate binding also exhibits some negative cooperativity in mGluR1 dimers, but this effect is ameliorated somewhat in the presence of millimolar levels of calcium (Suzuki et al., 2004). However, there are currently few studies addressing the issue of crosstalk within an mGluR1 dimer. For example, Can glutamate activate the mGluR1 dimer by binding at only one subunit? This issue has been difficult to resolve in part due to the lack of a verifiably monomeric mGluR1 mutant. The cysteine at position 140 of mGluR1 is known to form a disulfide bond covalently linking mGluR1 dimers (Robbins et al., 1999; Kunishima et al., 2000; Ray and Hauschild, 2000), but mutation of this residue does not exclude dimer formation, as non-covalently bound dimers are observed (Tsuji et al., 2000).

In this study, the importance of mGluR1 intra-dimer interaction was examined. Specifically, the questions addressed were: does each individual receptor within an mGluR1 dimer molecule function independently? If not, what is the nature of the interaction? These questions were addressed by measuring glutamate-mediated calcium current modulation, and by constructing concentration-response curves in rat sympathetic neurons from the superior cervical ganglion (SCG) heterologously expressing mGluR1 and mGluR1 Y74A, a mutant with impaired glutamate binding (Sato, et al). In addition, the glutamate dose-response curves were examined under conditions designed to observe activity of heterodimers of the wild-type (WT) mGluR1 and the Y74A mutant.

METHODS

Cell isolation, DNA injection and Plasmids

A detailed description of the cell isolation and cDNA injection protocol can be found elsewhere (Ikeda, 1997). Animal protocols were approved by the Institutional Animal Care and Use Committee (IACUC). Briefly, both SCGs were removed from adult male Wistar rats (175-225 g) following CO₂ euthanasia and decapitation, and incubated in Earle's balanced salt solution (InVitrogen, Life Technologies Carlsbad, CA) containing 0.55 mg ml⁻¹ trypsin (Worthington Biochemicals, Freehold, NJ) and 0.7 mg ml⁻¹ collagenase D (Boehringer Mannheim Biochemicals, Indianapolis, IN) for 1 hour at 35 °C. Cells were then transferred to minimum essential medium (InVitrogen/Gibco), plated on poly-L-lysine (Sigma Chemical Co., St. Louis, MO) coated 35 mm polystyrene tissue culture dishes and incubated (95% air and 5% CO₂; 100% humidity) at 37 °C prior to DNA injection. Following injection, cells were incubated overnight at 37 °C and patch clamp or immunofluorescence experiments were performed the following day.

Injection of cDNA was performed with an Eppendorf 5247 microinjector and InjectMan NI 2 micromanipulator (Madison, WI) 4-6 hours following cell isolation. Injection electrodes were made with a Sutter P-97 horizontal electrode puller (Novato, CA) using thin-walled, borosilicate glass (World Precision Instruments, Sarasota, FL). Plasmids were stored at -20 °C as a 1 µg µl⁻¹ stock solution in TE buffer (10 mM TRIS, 1 mM EDTA, pH 8). mGluR1 constructs were injected at 50-100 ng µl⁻¹, as indicated (pCDNA3.1⁺; InVitrogen). The Y74A mutant was produced using the QuikChange Site-Directed Mutagenesis strategy (Stratagene), using complimentary primers (forward sequence: 5'- gt ggg gag atc agg gaa cag GCt ggt atc cag agg gtg gag gcc atg; capital letters indicate base changes). Wild type mGluR1 and myc-mGluR1 (pCDNA3.1+) were used as the templates for the QuikChange reaction. The myc-mGluR1 construct was

made using the overlap extension PCR technique (Ho et al., 1989). The myc sequence *GAA CAA AAA CTC ATC TCA GAA GAG GAT CTG* was inserted after amino acid 34 of mGluR1. All neurons were co-injected with “enhanced” green fluorescent protein cDNA (0.005 $\mu\text{g } \mu\text{l}^{-1}$; pEGFP-N1; BD Biosciences-Clontech, Palo Alto, CA) to facilitate identification of successfully injected cells.

All constructs were sequence confirmed (Fisher-SeqWright, Houston, TX). PCR products were purified with Qiagen (Valencia, CA) silica membrane spin columns prior to restriction digestion and ligation. Plasmids were propagated in the Top10 *E. coli* strain (Invitrogen) and midpreps were prepared using Qiagen anion exchange columns.

Electrophysiology and data analysis

Patch pipettes were made with a Sutter P-97 horizontal puller from 8250 glass (Garner Glass, Claremont, CA) and had resistances of 1-3 M Ω . Series resistances were 2-5 M Ω prior to electronic compensation of 80%. Whole-cell patch-clamp recordings were made with an Axopatch 200B patch clamp amplifier (Axon Instruments, Foster City, CA). Voltage protocol generation and data acquisition were performed using custom software (courtesy Stephen R. Ikeda, NIAAA, Rockville, MD) on a Macintosh G3 computer (Apple Computer, Cupertino, CA) with an InstruTech (Port Washington, NY) ITC-18 data acquisition board. Currents were low-pass filtered at 5 kHz using the 4-pole Bessel filter in the patch clamp amplifier, digitized at 2-5 kHz and stored on the computer for later analysis. Experiments were performed at 21-24 °C (room temperature). Patch-clamp data analysis was performed using Igor Pro software (Wavemetrics, Lake Oswego, OR).

The external (bath) solution for patch-clamp recordings contained (in mM): 155 tris hydroxymethyl aminomethane, 20 4-(2-Hydroxyethyl)-1-piperazineethanesulfonic acid (HEPES), 10 glucose, 10 CaCl₂, and 0.0003 tetrodotoxin (TTX), pH 7.4. The internal (pipette) solution contained: 120 N-methyl-D-glucamine (NMG) methanesulfonate, 20

TEA, 11 EGTA, 10 HEPES, 10 sucrose, 1 CaCl₂, 4 MgATP, 0.3 Na₂GTP, and 14 tris creatine phosphate, pH 7.2. 100 μM L-Glutamate (Sigma) was used as the agonist for mGluR1. All drugs and control solutions were applied to cells using a custom, gravity-driven perfusion system positioned ~100 μm from the cell that allowed rapid solution exchange (≤ 250 ms). The degree of mGluR-mediated calcium current inhibition was calculated as the maximal inhibition of the current in the presence of drug compared to the last current measurement prior to application of the drug.

Immunofluorescence experiments

To detect surface expression of the mGluR1-myc construct, a cy3-conjugated, mouse anti-myc, monoclonal antibody (Sigma) was applied to live cells at room temperature for 25 minutes at a 1:150 dilution. Cells were subsequently washed five times in phosphate buffered saline (PBS) and images were acquired from live cells. Images were taken using a Spot 2, cooled CCD camera (Diagnostic Instruments, Inc., Sterling Heights, MI) mounted onto a Nikon Y-FL upright microscope with a 60X, water immersion objective (Nikon). Fluorescence images were obtained using Spot software (Diagnostic Instruments) and figures were constructed using Adobe Photoshop (Adobe Systems Inc., San Jose, CA) and Canvas (ACD Systems of America, Inc., British Columbia, Canada.) software. Quantitative image analysis was performed using NIH Image software. All images analyzed for Figure 6 were obtained using identical conditions (exposure time, gain, etc.), chosen to put the majority of cells' fluorescence near the center of the camera's dynamic range. Using 8 bit images, total fluorescence of a small area encompassing the entire cell was measured and the fluorescence of an identically sized area of background was subtracted to yield a measure of total fluorescence for each cell.

Western blots

18-24 hours after transfection, HEK293 cells were washed twice with ice-cold phosphate buffered saline (PBS) and incubated in lysis buffer (0.5% TritonX-100, 1 mM EDTA, 1 mM iodoacetamide in PBS) plus protease inhibitors (Sigma) for 15 min at 4 °C. Lysates were collected by centrifuging cells at 16,000 xg for 10 min at 4 °C. Protein concentration was determined by Bradford assay. 30 µg of cell lysate was treated with 2x Laemmli sample buffer. Samples were incubated at room temperature for 10 min prior to electrophoresis. Cell lysates were separated on a 6 % SDS-polyacrylamide gel with a 3 % stacker, and transferred to PVDF membranes. PVDF membranes were blocked in 5 % milk and incubated in anti-mGluR1 (0.25 µg/ml, Upstate) for 1 hr. Blots were washed with TBS-Tween (0.05 %) and incubated with anti-rabbit secondary antibody conjugated to horseradish peroxidase (1:3000). Signals were detected by enhanced chemiluminescence (Pierce).

RESULTS

Glutamate dose-response for mGluR1 expressed in SCG neurons

Isolated SCG neurons do not express functional mGluRs (Ikeda et al., 1995). However, mGluR1 expressed heterologously in SCG neurons has been shown to negatively couple to the predominantly N-type (Zhu and Ikeda, 1994) native calcium channels through activation of both pertussis toxin sensitive and insensitive G proteins (Kammermeier and Ikeda, 1999). This calcium current inhibitory response was used to test the effect of glutamate (Glu) on mGluR1 expressed in SCG neurons. Figure 1Aa illustrates the time course of calcium current amplitude in such a cell exposed to various concentrations of Glu. A standard triple pulse voltage protocol was used to assess the current amplitude in these experiments (Elmslie et al., 1990). Using the whole-cell patch-clamp configuration, cells were held at -80 mV then stepped every 10 seconds to $+10$ mV for 25 msec (the prepulse; “pre” in Figure 1A). Next, a 50 msec depolarizing step to $+80$ mV was given to induce facilitation of the $G\beta\gamma$ -mediated, PTX sensitive calcium current inhibition (Herlitze et al., 1996; Ikeda, 1996), and after a brief, 10 msec step back to -80 mV a second test pulse to $+10$ mV was applied (the postpulse; “post” in Figure 1A). Figure 1Ab illustrates control and $30\ \mu\text{M}$ Glu-inhibited currents from the cell shown in Figure 1Aa. The Glu-mediated inhibition of the calcium current is rapid and reversible.

The average (\pm SEM, $n=6$ cells) dose-response data for wild type mGluR1 is illustrated in Figure 1B (*filled circles*). The data indicate that $0.1\ \mu\text{M}$ Glu is sub-threshold, and that the response begins to saturate around $10\ \mu\text{M}$. The data were fit to a single-site binding isotherm equation (see figure legend), which appeared to provide an adequate fit to the data. The IC_{50} was determined to be approximately $1.3\ \mu\text{M}$. Maximal inhibition (I_{MAX}) of calcium current in SCG neurons via mGluR1 was $64\pm 3\%$ (inhibition at $100\ \mu\text{M}$). In addition to the wt mGluR1, a dose-response curve was generated for an

N-terminally myc-tagged mGluR1 (myc-mGluR1; *open circles* in Figure 1B). The IC_{50} and I_{MAX} of Glu were $1.7 \mu M$ and $62 \pm 6\%$ ($n=6$), respectively. These values were similar to those obtained from the wild-type mGluR1.

These data show that mGluR1 expressed in SCG neurons initiates calcium current inhibition with an IC_{50} in the low micromolar range. In addition, insertion of the extracellular myc-tag into the mGluR1 sequence does not appear to alter Glu binding or receptor activation.

Effect of the Y74A point mutation on the Glu dose-response

Structural studies indicate that the tyrosine residue at position 74 in mGluR1 (Y74) contacts Glu in the extracellular binding domain (Kunishima et al., 2000; Sato et al., 2003). Further, mutation of this residue to alanine (Y74A) disrupts Glu binding to the pocket (Sato et al., 2003). Results here confirmed this finding. Figure 2Aa shows the time course for the calcium current inhibitory responses to various concentrations of Glu for a cell expressing mGluR1 Y74A. Control and 1 mM inhibited current traces are also shown for this cell (Figure 2Ab). The average dose-response data from mGluR1 Y74A (and for WT mGluR1, for contrast) are illustrated in Figure 2B ($n=9$ mGluR1 Y74A cells; wild-type data is identical to that in Figure 1B). Glu concentrations up to and including $100 \mu M$ were without effect, although application of 1-10 mM Glu produced potent inhibition (Figure 2B, *open circles*; $n=12$). Uninjected cells exposed to 1-10 mM Glu showed no inhibition (Figure 2B, *triangles*; $n=6$). The mGluR1 Y74A I_{MAX} value was slightly larger than the maximal inhibition observed with the wt mGluR1 constructs, suggesting that Glu can bind the Y74A mutant and activate the receptor, but with much lower apparent affinity. The approximate IC_{50} for Glu acting on mGluR1 Y74A was $445 \mu M$. These data demonstrate that mutation of residue Y74 of mGluR1 to alanine produces an approximate shift in Glu affinity of >2 orders of magnitude, but without a reduction of I_{MAX} .

The function of mGluR1 Y74A-myc-mGluR1 dimers

To assess the signaling mechanism of mGluR1 wild type/Y74A heterodimers, dose-response curves for Glu were generated in cells injected with mGluR1 Y74A and myc-mGluR1 cDNA at a ratio of 2:1, respectively (see Figure 3A for a summary of expected ratios of expressed receptors). Two assumptions of these predictions are that the Y74A mutant expresses and can form dimers. The mutated residue resides deep within the binding pocket and is therefore not expected to influence dimerization. However, its ability to dimerize was nonetheless assessed by expressing each receptor in HEK293 cells and performing western blots on the resulting proteins using an anti-mGluR1 antibody. Figure 3C illustrates that mGluR1 Y74A dimerization (center column) does not appear to be compromised. In addition, a mutant known to form only non-covalent dimers, mGluR1 C140A, was also examined as a negative control (right column). This mutant showed clearly impaired dimerization. Thus, the mGluR1 Y74A mutant appears to exhibit unimpaired dimerization. Although these data do not directly address the assumptions of Figure 3A and B by providing direct measurements of wild type/mutant heterodimer formation, they do provide supporting evidence that a change in the ability of the Y74A mutant to dimerize is unlikely.

Figure 4Aa shows the time course of the calcium current inhibitory responses for a cell expressing mGluR1 Y74A and wild type at a 2:1 ratio (as in Figure 3A). Note that 100 μ M Glu produced only a small inhibition of the calcium current, while lower concentrations produced no effect. Sample current traces in control and 1 mM Glu are shown in Figure 4Ab. Figure 4B shows the average (\pm SEM) responses over the entire range of doses tested for cells expressing 2:1 mGluR1 Y74A:myc-mGluR1 (*solid squares*). Also shown are the dose-response curves for wt mGluR1 alone (*open circles*), myc-mGluR1 alone (*solid circles*) and mGluR1 Y74A alone (*open squares*) for comparison. Note that the absolute myc-mGluR1 cDNA concentration injected in both experiments (2:1 Y74A:myc-mGluR1 and myc-mGluR1 alone) were identical (50 ng/ μ l).

Calcium current inhibition at 1 mM Glu for the 2:1 mGluR1 Y74A:myc-mGluR1 cells was $58 \pm 9\%$ ($n=8$). Indeed, at every concentration tested, the Glu response in cells expressing 2:1 mGluR1 Y74A:myc-mGluR1 was similar that in cells expressing mGluR1 Y74A alone (with the exception of the super-saturating concentrations > 1 mM; Figure 4B). The lack of effect in this concentration range demonstrates that the population of WT homodimers is too small to produce a detectable signal, provided the wild type construct's expression is verified (see below). In addition, WT/Y74A heterodimers appear unable to couple to G protein in this concentration range despite the presence of a binding site expected to interact with Glu (i.e. the WT subunit). These data support a model in which mGluR1 dimers are inactive when bound to a single Glu ligand. However, before this conclusion was embraced, the constructs were expressed at the inverse ratio (see Figure 3B) to determine if they behave as predicted by this interpretation. Finally, the possibility that expression of mGluR1 Y74A occludes expression of myc-mGluR1 was tested.

The Y74A mutant and mGluR1 WT cDNA were injected in SCG neurons at a ratio of 1:2 (mGluR1 Y74A:myc-mGluR1 WT, respectively; Figure 5). Calcium current inhibitory responses to a range of Glu concentrations (injected with 100 ng/ μ l myc-mGluR1 and 50 ng/ μ l mGluR1 Y74A) for such a cell are shown in Figure 5A. In this cell, there is clearly a high-potency component (note the small inhibition at 3 μ M and the larger inhibition at 10 and 100 μ M). In addition, the calcium current inhibition appears to be increased when the Glu concentration is increased to 1 mM. These data are summarized in Figure 5B (*open squares with X*), and contrasted to data from cells expressing myc-mGluR1 alone (*solid circles*) and both myc-mGluR1 and mGluR1 Y74A at a 2:1 ratio (*open squares*). Cells expressing 1:2 myc-mGluR1 and mGluR1 Y74A were inhibited $44 \pm 7\%$ at 100 μ M and $61 \pm 5\%$ at 1 mM ($n=12$). These data imply that myc-mGluR1 expression is not occluded in the presence of the mGluR1 Y74A construct. In

addition, the data in Figure 4 support a model in which mGluR1 dimers require two bound glutamates for activation.

Expression of myc-mGluR1 Y74A

To determine whether myc-mGluR1 expression was altered in the presence of mGluR1 Y74A, surface expression of myc-mGluR1 was assessed when this construct was expressed alone or in combination with the Y74A mutant as in the experiment described above (Figure 4). Surface expression was quantified by exposing live cells to a cy3-conjugated, anti-myc monoclonal antibody directed against the receptor's external myc epitope, and measuring average fluorescence for each expression condition (see *Experimental Procedures* for details). Figure 6Aa shows examples of an SCG neuron expressing myc-mGluR1 alone (50 ng/ μ l cDNA injected). The images illustrate bright field, GFP fluorescence (co-injected to identify expressing cells) and cy3 fluorescence. Figure 6Ab is similar, but from a cell expressing myc-mGluR1 (50 ng/ μ l cDNA injected) plus mGluR1 Y74A (100 ng/ μ l cDNA injected). A summary of the data (Figure 6B) shows average cy3 fluorescence for cells expressing myc-mGluR1 alone (32 ± 11 , arbitrary fluorescence units, $n=4$, *open bar*), cells expressing both myc-mGluR1 and mGluR1 Y74A (33 ± 11 , $n=4$, *solid bar*), and for 6 uninjected cells (10 ± 2 , *hatched bar*). These data indicate that surface expression of myc-mGluR1 is not altered within the limits of immunofluorescence detection when co-expressed with mGluR1 Y74A, under conditions similar to that in the experiment described above (see Figures 3A and 4). Further, from the surface expression data described here and the dose-response data described in Figure 4 it can be inferred that there are substantial numbers of myc-mGluR1/mGluR1 Y74A heterodimers present under the conditions described above (Figure 4), since the presence of myc-mGluR1 homodimers would presumably lead to calcium current inhibition at moderate Glu concentrations (1-100 μ M). Therefore, these

data support the model described above, in which mGluR1-mediated G protein activation requires that both dimer subunits bind Glu.

DISCUSSION

Data presented in this study suggest that mGluR1 dimers require glutamate at both subunits for receptor activation. Following co-expression of mGluR1 with mGluR1 Y74A, a mutant with impaired glutamate binding capability (Sato et al., 2003), activity of the resulting heterodimer (mutant/wild type) was examined by expressing the constructs at various ratios (excess mutant or excess wild type). Glutamate-mediated calcium current inhibition in sympathetic neurons from the rat SCG was examined to assess receptor activity. The data indicate that at glutamate concentrations that activate wild type mGluR1, but insufficient to activate mGluR1 Y74A, the mutant/wild-type heterodimer was inactive. Thus, mGluR1 dimers appear to exhibit intradimer interaction such that glutamate bound to a single subunit of the dimer is insufficient to activate the receptor (Figure 7).

The large shift in Glu affinity of the Y74A mutant provided an opportunity to investigate the role of dimerization in coupling mGluR1 to G protein activation. One possibility was that each molecule in the dimer acted independently. Although this model cannot be ruled out with available data, recent structural work suggests that the ligand binding regions act allosterically (Jingami et al., 2003) and that at least some cooperativity between subunits occurs (Suzuki et al., 2004), making the independent model seem unlikely.

Alternatively, the activation state of one mGluR1 subunit may be dependent on the glutamate bound to the other subunit. An example of this type of model is one in which a single bound glutamate was sufficient to activate the dimer pair, similar to the crosstalk of GABA_B receptors (Margeta-Mitrovic et al., 2001b). Alternatively, Glu binding to one dimer subunit may be insufficient to activate that receptor (i.e. promote GTP/GDP exchange) without Glu binding in the other partner as well. That is, the active state may

only be achieved when *both* dimer subunits are bound to Glu. One prediction of this model is that activation of mGluR1 ‘heterodimers’ (mGluR1 WT/Y74A heterodimers) is limited by the low affinity partner. The independent model would conversely predict that the dose-response curve of a ‘heterodimer’ population would have two components: a low and a high affinity component wherein at least some response would be seen at lower concentrations.

To perform this experiment was problematic. Since each receptor (mGluR1 and mGluR1 Y74A) can form stable homodimers, a pure ‘heterodimer’ population cannot be achieved. When both receptors are expressed in a cell, the resulting population of mGluR dimers will be composed of three forms of dimer: wild type (WT) homodimers, WT/Y74A ‘heterodimers’, and Y74A homodimers. Proportions of each dimer form depend on the relative levels of each receptor (WT and Y74A). Assuming that homo- or heterodimers form equally well (see Figure 3C), one can predict that with equal levels of each construct, half of the existing dimers will be WT/Y74A heterodimers, while each homodimer will constitute one quarter of the population. If the mutant and wild type receptors are expressed at a 2:1 ratio, only about 1 in 9 receptors will be wild type homodimers, while the remainder should be equal numbers of mutant homodimers and heterodimers (Figure 3A). Conversely, with the ratio reversed a minimal number of mutant homodimers are expected while heterodimers and wild type homodimers should predominate (Figure 3B), provided the relationship between cDNA injected and protein expressed is similar for the two constructs. This seems likely since these constructs are nearly identical (the two plasmid constructs differ at only 32 of about 9000 bases, including the myc insert). However, it is not critical that protein levels exactly correlate with cDNA ratios injected, provided the mutant is expressed at higher levels such that few WT homodimers form, but enough WT mGluR1 protein is expressed that the heterodimer population is detectable. Fortunately, both of these assumptions could be tested (see Figures 5 and 6).

Conclusions from the data in this study also rely on the assumption that the Y74A mutation impairs glutamate affinity without appreciably altering the activation process. This assumption is crucial because in this study, only downstream signaling of mGluR1 can be measured. Secondary effects of the mutation unrelated to glutamate binding may be undetectable. Two lines of evidence indicate that the Y74A mutation does not detrimentally affect receptor activation. First, if the receptor activation process were impaired in mGluR1 Y74A, activation would be altered in response to all agonists. However, activation by the agonist quisqualate, as well as quisqualate binding, appears unaffected by the mutation (Sato et al., 2003). Since the Y74 residue is known to contact glutamate but not quisqualate in the binding pocket, this finding was expected (Kunishima et al., 2000).

Second, the maximal effect of mGluR1 Y74A in SCG neurons was not reduced (in fact, it was slightly increased) compared to the wild type mGluR1 (Figure 4). In addition, calcium current modulation observed via mGluR1 Y74A was qualitatively similar to that induced by the wild-type mGluR1. Voltage dependence of the modulation, an estimate of the relative contribution of the pertussis toxin-sensitive and insensitive components of inhibition (Kammermeier and Ikeda, 1999) were indistinguishable (not shown). Thus, it appears that the Y74A mutation impairs glutamate binding but not receptor activation *per se*.

A final assumption of this study is that the Y74A mutation has unimpaired ability to dimerize. The Y74 residue of mGluR1 resides in the interior of the binding pocket, a relatively large distance from the dimer interface (Kunishima et al., 2000; Sato et al., 2003), so disruption of dimerization is not expected. Further, the experiments in Figure 4 provide evidence that mGluR1 Y74A can dimerize with the wild type mGluR1. Expression of myc-mGluR1 does not appear to change within the limits of immunofluorescence detection when co-expressed with excess mGluR1 Y74A compared to when expressed alone. Thus, if mGluR1 Y74A was unable to dimerize with the wild

type mGluR1, some modulation of calcium current should have been detectable between 1 and 100 μ M when the two constructs were co-expressed (as in Figure 4). Nonetheless, the ability of the mGluR1 Y74A mutant to dimerize was directly tested by western blotting of expressed receptor in HEK293 cells. The mutant's ability to form dimers was not detectably impaired compared to the wild type mGluR1 (see Figure 3C).

Activation of mGluR1 results from a complex series of conformational changes in the N-terminus of the receptor (Jingami et al., 2003). Each mGluR1 protomer in the dimer forms a bi-lobed structure. Glutamate binding at each protomer stabilizes the closed state of the binding pocket. In addition, a further shift of each subunit relative to the other is observed in the presence of glutamate, which moves the dimer from the so-called "R" to the "A" conformation. Thus, an inactive, or 'resting' receptor is likely one that is unbound to glutamate and predominantly occupies the open-open/R conformation at equilibrium. By contrast, an 'active' receptor appears to be one in which two glutamate ligands are bound (one to each dimer subunit) with equilibrium favoring either an open-closed/A conformation or a closed-closed/A conformation, perhaps depending on the presence of calcium or gadolinium (Tsuchiya et al., 2002). Indeed, a recent study indicates that the closed/closed state appears to permit greater receptor activity than the open/closed state, supporting the results observed here (Kniazeff et al., 2004). Although it is impossible to deduce structural information from the physiological data presented in this study, the lack of receptor signaling seen here suggest that under the artificial conditions imposed (of a WT/Y74A heterodimer presumably bound to a single Glu ligand), mGluR1 occupies a resting, or 'R' conformation.

It is interesting to speculate on an alternative to the interpretation proposed above, that an mGluR1 dimer bound to a single Glu ligand results in an inactive receptor (as in Figure 7). Namely, that the lack of mGluR1 WT/Y74A heterodimer signaling at moderate Glu concentrations observed in this study may imply that Glu is unable to bind the WT subunit of the heterodimer when the mutant subunit is ligand-free. This alternate

interpretation is also consistent with the physiological data presented here. Both interpretations support the conclusion that some form of intra-molecular crosstalk occurs within mGluR1 dimers. In both cases, ligand bound to a single mGluR1 subunit influences the ability of the receptor dimer to couple to G protein. Although glutamate binding can neither be measured in single SCG neurons nor in other cells on a comparable time scale to that of this study, the latter interpretation amounts to positive cooperativity in mGluR1 dimers. Since only negative cooperativity has been observed in mGluR1 (Suzuki et al., 2004), this model was not considered further.

In summary, co-expression of WT mGluR1 with mGluR1 Y74A, a mutant with impaired glutamate binding, was used to examine signaling of the WT/mutant heterodimer. This heterodimer was inactive at glutamate concentrations below $\sim 100 \mu\text{M}$, a concentration range at which one subunit of the dimer (the WT) is expected to bind Glu. Thus, intramolecular crosstalk appears to occur in mGluR1 dimers such that the receptors require glutamate at both subunits to activate the G protein-mediated pathway that results in ion channel modulation in neurons.

ACKNOWLEDGMENTS

I thank Elena Bocola-Mavar for valuable technical assistance and Stephen R. Ikeda for advice and for providing clones. I also thank Mark A. Simmons for helpful discussions.

REFERENCES

- Conn PJ and Pin JP (1997) Pharmacology and functions of metabotropic glutamate receptors. *Annu Rev Pharmacol Toxicol* **37**:205-237.
- Elmslie KS, Zhou W and Jones SW (1990) LHRH and GTP- γ -S modify calcium current activation in bullfrog sympathetic neurons. *Neuron* **5**:75-80.
- Herlitze S, Garcia DE, Mackie K, Hille B, Scheuer T and Catterall W (1996) Modulation of Ca²⁺ channels by G-protein $\beta\gamma$ subunits. *Nature* **380**:258-262.
- Ho SN, Hunt HD, Horton RM, Pullen JK and Pease LR (1989) Site-directed mutagenesis by overlap extension using the polymerase chain reaction. *Gene* **77**:51-59.
- Ikeda SR (1996) Voltage-dependent modulation of N-type calcium channels by G-protein $\beta\gamma$ subunits. *Nature* **380**:255-258.
- Ikeda SR (1997) Heterologous expression of receptors and signaling proteins in adult mammalian sympathetic neurons by microinjection., in *Methods in Molecular Biology* (Challis RAJ ed) pp 191-202, Humana Press, Inc., Totowa, NJ.
- Ikeda SR, Lovinger DM, McCool BA and Lewis DL (1995) Heterologous expression of metabotropic glutamate receptors in adult rat sympathetic neurons: subtype-specific coupling to ion channels. *Neuron* **14**:1029-1038.
- Jingami H, Nakanishi S and Morikawa K (2003) Structure of the metabotropic glutamate receptor. *Curr Opin Neurobiol* **13**:271-278.
- Kammermeier PJ and Ikeda SR (1999) Expression of RGS2 alters the coupling of metabotropic glutamate receptor 1a (mGluR1a) to M-type K⁺ and N-type Ca²⁺ channels. *Neuron* **22**:819-829.
- Kaupmann K, Huggel K, Heid J, Flor PJ, Bischoff S, Mickel SJ, McMaster G, Angst C, Bittiger H, Froesti W and Bettler B (1997) Expression cloning of GABA_B

- receptors uncovers similarity to metabotropic glutamate receptors. *Nature* **386**:239-246.
- Kniazeff J, Bessis AS, Maurel D, Ansanay H, Prezeau L and Pin JP (2004) Closed state of both binding domains of homodimeric mGlu receptors is required for full activity. *Nat Struct Mol Biol* **11**:706-713.
- Kunishima N, Shimada Y, Tsuji Y, Sato T, Yamamoto M, Kumasaka T, Nakanishi S, Jingami H and Morikawa K (2000) Structural basis of glutamate recognition by a dimeric metabotropic glutamate receptor. *Nature* **407**:971-977.
- Margeta-Mitrovic M, Jan YN and Jan LY (2000) A trafficking checkpoint controls GABA(B) receptor heterodimerization. *Neuron* **27**:97-106.
- Margeta-Mitrovic M, Jan YN and Jan LY (2001a) Function of GB1 and GB2 subunits in G protein coupling of GABA(B) receptors. *Proc Natl Acad Sci U S A* **98**:14649-14654.
- Margeta-Mitrovic M, Jan YN and Jan LY (2001b) Ligand-induced signal transduction within heterodimeric GABA(B) receptor. *Proc Natl Acad Sci U S A* **98**:14643-14648.
- Nakanishi S (1994) Metabotropic glutamate receptors: synaptic transmission, modulation and plasticity. *Neuron* **13**:1031-1037.
- Pin J-P and Duvoisin R (1995) Neurotransmitter receptors I. The metabotropic glutamate receptors: structure and functions. *Neuropharmacology* **34**:1-26.
- Ray K and Hauschild BC (2000) Cys-140 is critical for metabotropic glutamate receptor-1 dimerization. *J Biol Chem* **275**:34245-34251.
- Robbins MJ, Calver AR, Filippov AK, Hirst WD, Russell RB, Wood MD, Nasir S, Couve A, Brown DA, Moss SJ and Pangalos MN (2001) GABA(B2) is essential for g-protein coupling of the GABA(B) receptor heterodimer. *J Neurosci* **21**:8043-8052.

- Robbins MJ, Ciruela F, Rhodes A and McIlhinney RA (1999) Characterization of the dimerization of metabotropic glutamate receptors using an N-terminal truncation of mGluR1alpha. *J Neurochem* **72**:2539-2547.
- Romano C, Yang WL and O'Malley KL (1996) Metabotropic glutamate receptor 5 is a disulfide-linked dimer. *J Biol Chem* **271**:28612-28616.
- Sato T, Shimada Y, Nagasawa N, Nakanishi S and Jingami H (2003) Amino acid mutagenesis of the ligand binding site and the dimer interface of the metabotropic glutamate receptor 1. Identification of crucial residues for setting the activated state. *J Biol Chem* **278**:4314-4321.
- Suzuki Y, Moriyoshi E, Tsuchiya D and Jingami H (2004) Negative cooperativity of glutamate binding in the dimeric metabotropic glutamate receptor subtype 1. *J Biol Chem*. **279**:35526-34.
- Tsuchiya D, Kunishima N, Kamiya N, Jingami H and Morikawa K (2002) Structural views of the ligand-binding cores of a metabotropic glutamate receptor complexed with an antagonist and both glutamate and Gd³⁺. *Proc Natl Acad Sci U S A* **99**:2660-2665.
- Tsuji Y, Shimada Y, Takeshita T, Kajimura N, Nomura S, Sekiyama N, Otomo J, Usukura J, Nakanishi S and Jingami H (2000) Cryptic dimer interface and domain organization of the extracellular region of metabotropic glutamate receptor subtype 1. *J Biol Chem* **275**:28144-28151.
- Zhu Y and Ikeda SR (1994) VIP inhibits N-type Ca²⁺ channels of sympathetic neurons via a pertussis toxin-insensitive by cholera toxin-sensitive pathway. *Neuron* **13**:657-669.

FOOTNOTES

* Supported by The American Heart Association, Ohio Valley Chapter BGIA grant #0365223B (PJK).

Reprint requests should be directed to:

Department of Physiology and Pharmacology
Northeastern Ohio Universities College of Medicine (NEOUCOM)
4209 State Route 44, PO Box 95
Rootstown, OH 44272

FIGURE LEGENDS

Figure 1. Glutamate dose-response curve for the modulation of calcium current by heterologously expressed mGluR1 in rat SCG neurons. Aa, Time course of calcium current inhibition by indicated concentrations of glutamate. Current measured from the prepulse (*solid circles*) and postpulse (*open circles*) are shown, using the triple pulse voltage protocol described in the text. Ab, Sample current traces before ('Control') and during ('30 μ M Glu') application of 30 μ M glutamate for the same cell shown in Aa. Scale bars represent 0.4 nA and 20 msec. B, Glutamate dose-response relationship showing average (\pm SEM) calcium current inhibition at seven points for SCG neurons expressing either mGluR1 (*solid circles*) or myc-mGluR1 (*open circles*). Estimated IC_{50} values for each group are shown below.

Figure 2. Glutamate dose-response curve for the mGluR1 Y74A mutant. Aa, Time course of calcium current inhibition by indicated concentrations of glutamate, as in Figure 1Aa. Ab, Sample current traces before ('Control') and during ('1 mM Glu') application of 1 mM glutamate for the same cell shown in Aa. Scale bars represent 0.4 nA and 20 msec. B, Glutamate dose-response relationship showing average (\pm SEM) calcium current inhibition at multiple points for SCG neurons expressing either mGluR1 (*solid circles*) or mGluR1 Y74A (*open circles*). Estimated IC_{50} value for mGluR1 Y74A is shown.

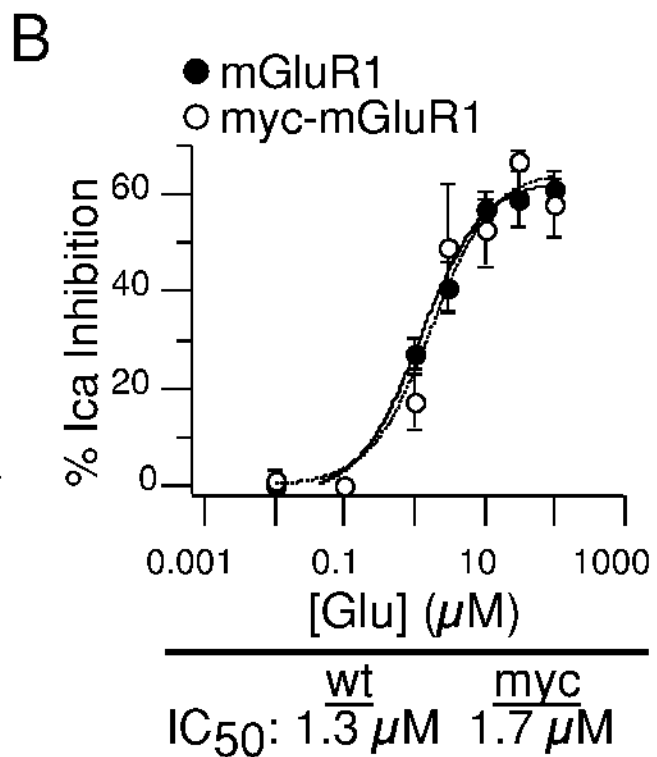
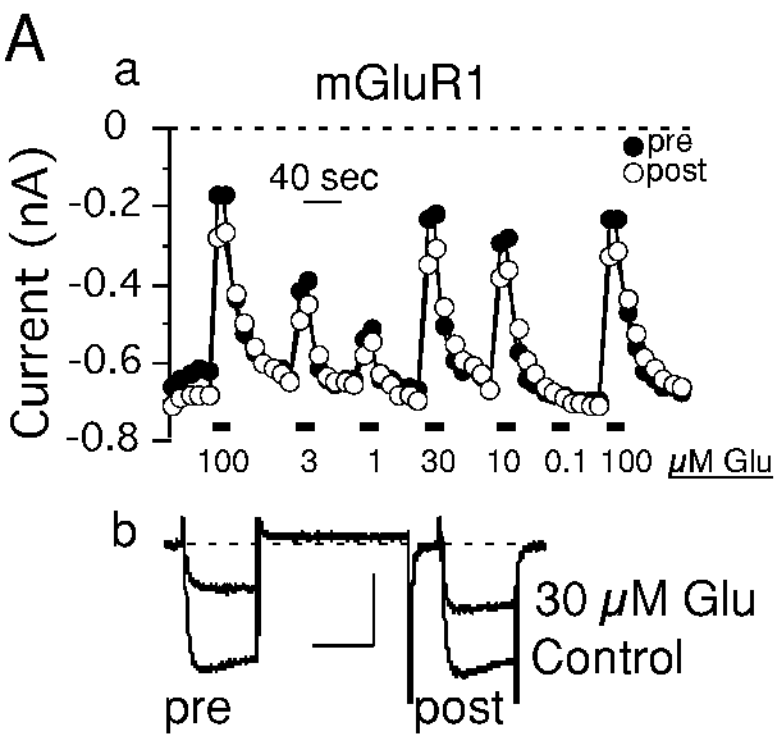
Figure 3. Schematic representation of the expected proportions of expressed dimeric receptors when mGluR1 Y74A and mGluR1 WT cDNA is injected at a 2:1 ratio (A) or a 1:2 ratio (B), as in subsequent experiments. C, Anti-mGluR1 western blot showing protein from HEK293 cells transfected with mGluR1 wild type, Y74A or C14A mutant as indicated.

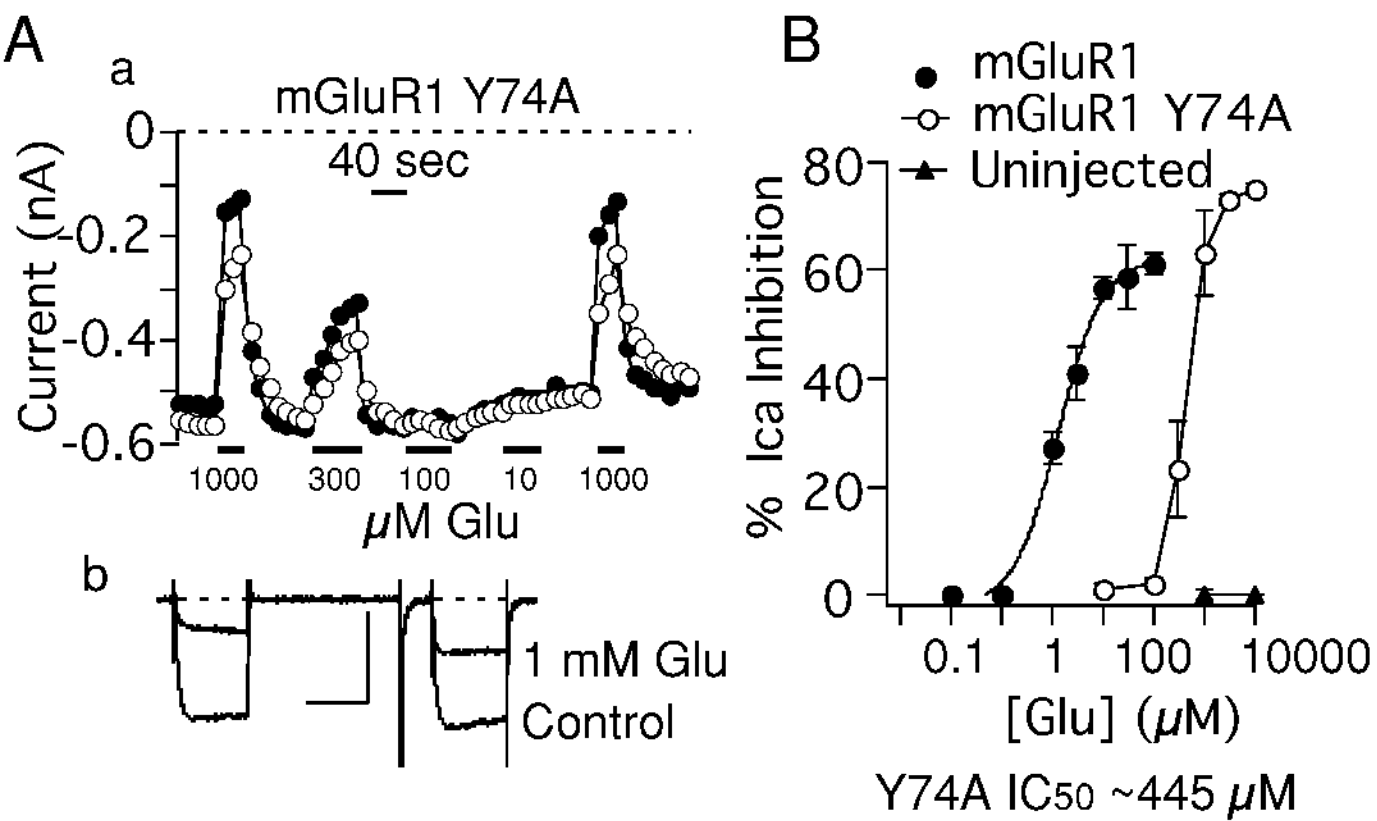
Figure 4. Glutamate dose-response curve for SCG neurons expressing a 2:1 ratio of mGluR1 Y74A and mGluR1 WT. Aa, Time course of calcium current inhibition by indicated concentrations of glutamate, as in Figure 1Aa. Ab, Sample current traces before ('Control') and during ('1 mM Glu') application of 1 mM glutamate for the same cell shown in Aa. Scale bars represent 0.4 nA and 20 msec. B, Glutamate dose-response relationship showing average (\pm SEM) calcium current inhibition at multiple points for SCG neurons expressing either mGluR1 (*open circles*), myc-mGluR1 (*solid circles*), mGluR1 Y74A alone (*open squares*), or mGluR1 Y74A and myc-mGluR1 at a 2:1 ratio (*solid squares*).

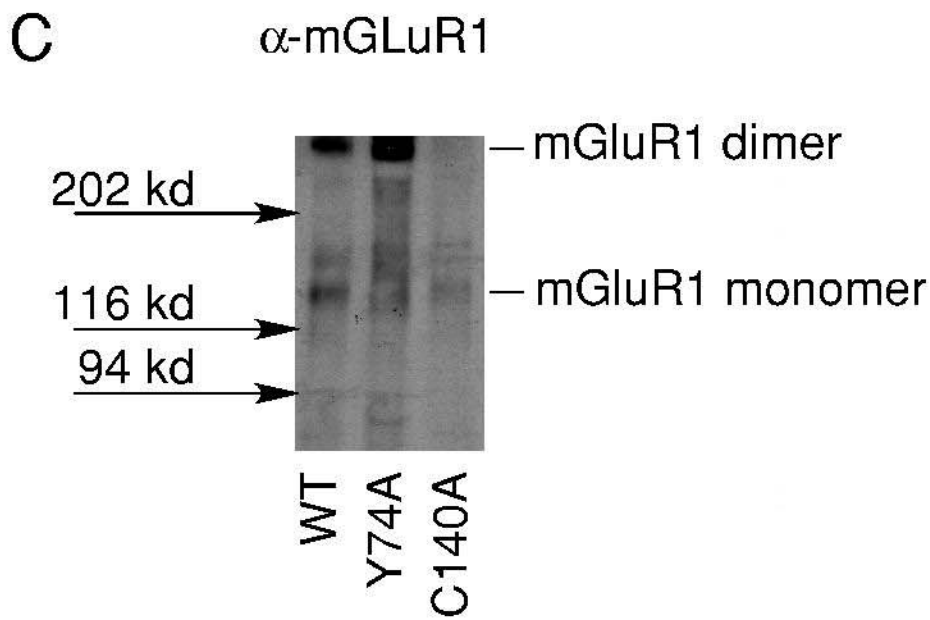
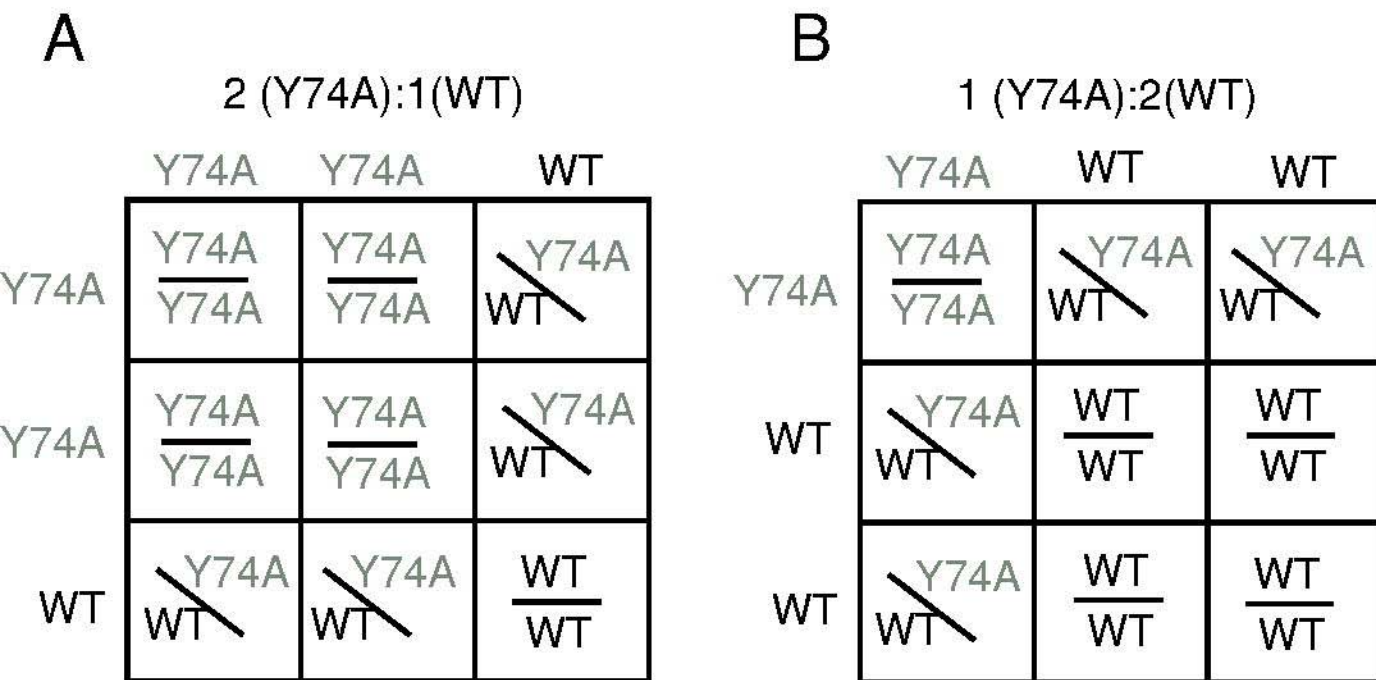
Figure 5. Glutamate dose-response curve for SCG neurons expressing a 1:2 ratio of mGluR1 Y74A and mGluR1 WT. A, Time course of calcium current inhibition by indicated concentrations of glutamate, as in Figure 1Aa. B, Glutamate dose-response relationship showing average (\pm SEM) calcium current inhibition at multiple points for SCG neurons expressing either mGluR1 (*open circles*), myc-mGluR1 (*solid circles*), mGluR1 Y74A and myc-mGluR1 at a 2:1 ratio (*open squares*), or at a 1:2 ratio (*open squares with X*).

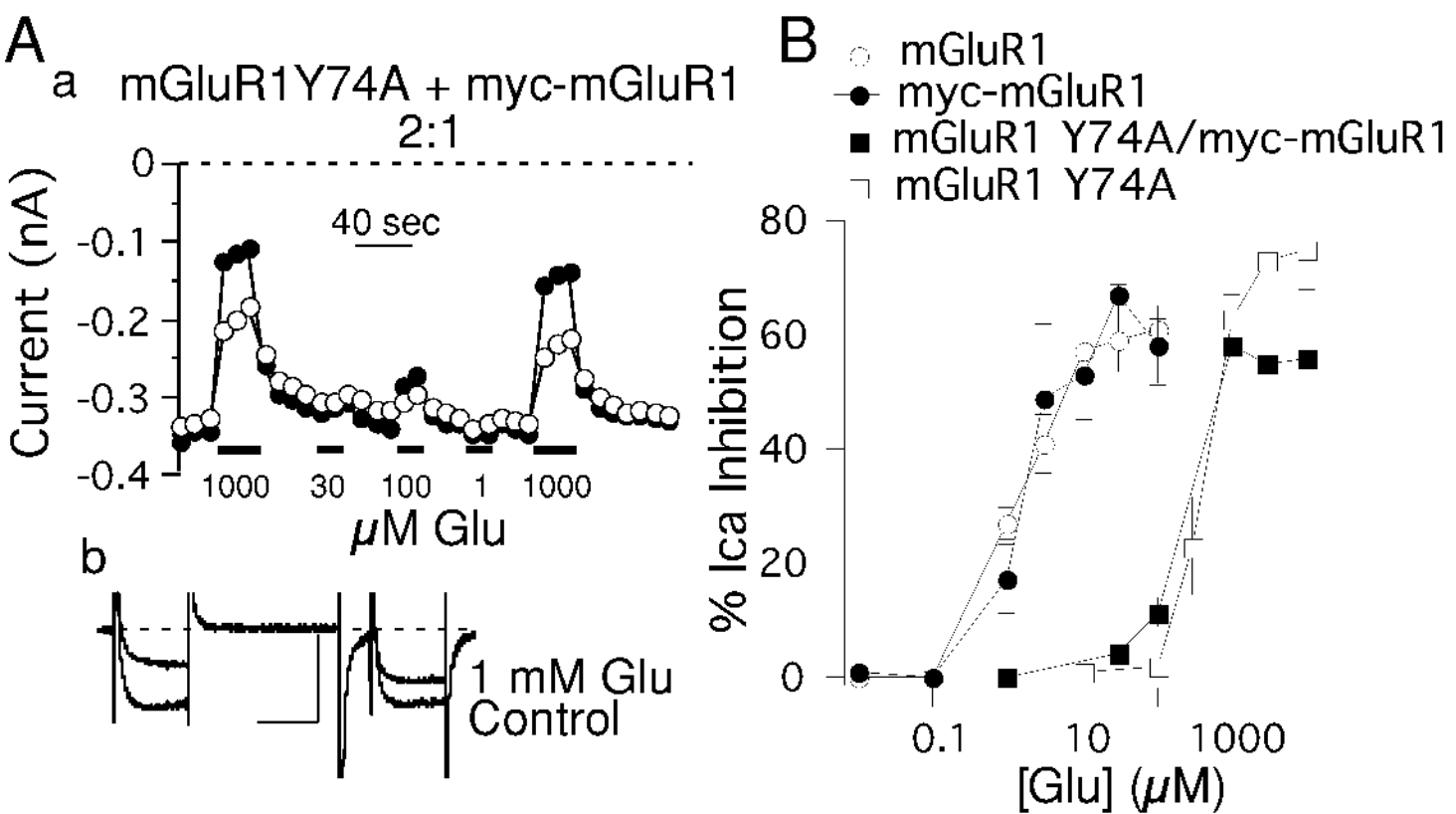
Figure 6. myc-mGluR1 expression is unaffected by co-expression of mGluR1 Y74A. Aa, Images showing bright field, GFP fluorescence and cy3 fluorescence of an SCG neuron expressing myc-mGluR1 alone and treated with cy3-conjugated, monoclonal anti-myc antibody. Ab, Images showing bright field, GFP fluorescence and cy3 fluorescence of an SCG neuron expressing mGluR1 Y74A and myc-mGluR1 at a 2:1 ratio and treated with cy3-conjugated, monoclonal anti-myc antibody. B, Average (+ SEM) cy3 fluorescence for SCG neurons expressing myc-mGluR1 (*open bar*), mGluR1 Y74A and myc-mGluR1 (*solid bar*) and for un-injected control cells (*hatched bar*), treated as in Aa, and b.

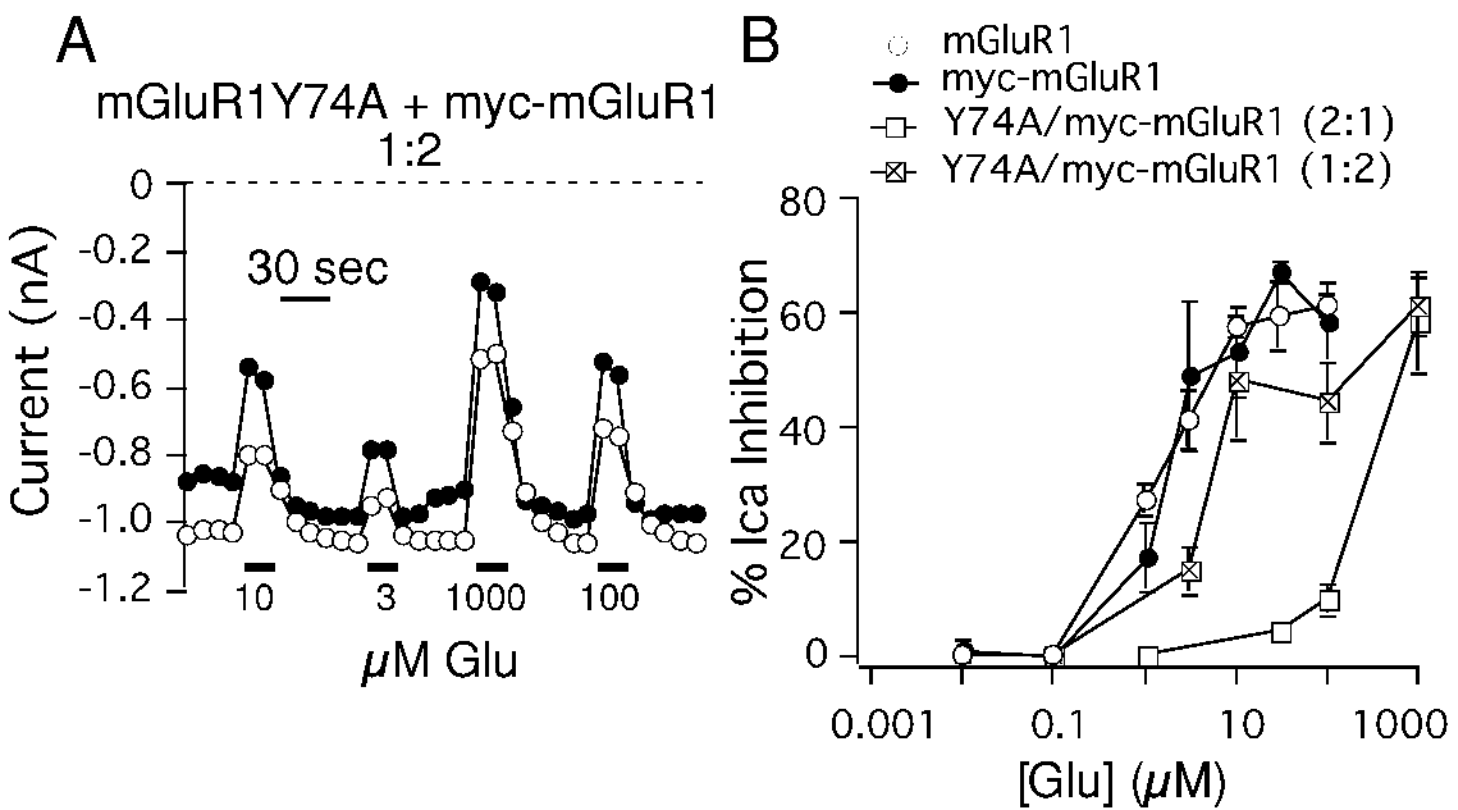
Figure 7. Schematic representation of mGluR1 dimer activation as a function of the number of glutamate ligands bound. This model is supported by data suggesting that WT/Y74A mGluR1 heterodimers are inactive at moderate glutamate concentrations at which only the WT subunit is expected to bind glutamate.

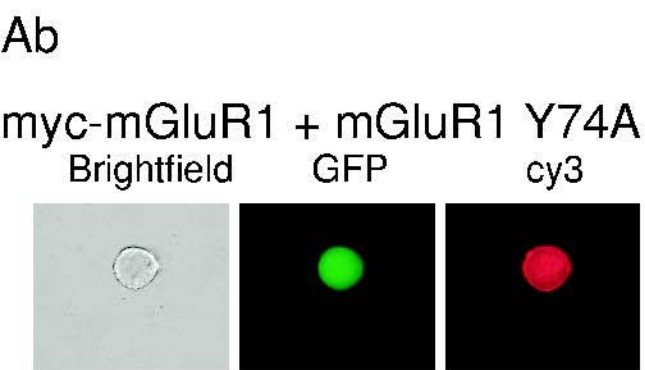
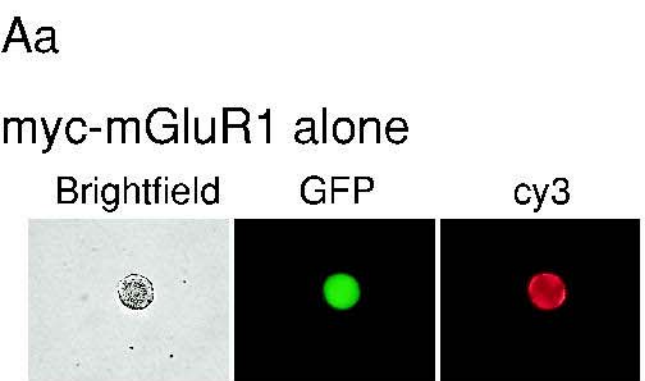












B

myc-mGluR1
myc-mGluR1 + Y74A
Uninjected

